JOURNAL OF CATALYSIS **172,** 170–177 (1997)
ARTICLE NO. CA971849

Quantification of Brønsted Acidity in Mordenites

M. A. Makarova,[1] A. E. Wilson, B. J. van Liemt, C. M. A. M. Mesters, A. W. de Winter, and C. Williams

Shell Research and Technology Center Amsterdam, P.O. Box 38000, 1030 BN Amsterdam, The Netherlands

Received April 16, 1997; revised July 15, 1997; accepted July 15, 1997

FTIR and NMR spectroscopy have been applied to quantification of Brønsted acid sites in various mordenite samples. A standardised deconvolution procedure has been developed for reliable decomposition of the complex hydroxyl region in the infrared spectra of mordenites into high frequency and low frequency peaks, and the peak extinction coefficients have been determined. As a result, the overall number of Brønsted acid sites, their distribution between main channels and side pockets, and the amount of extraframework aluminium can be determined. Results obtained by both FTIR and NMR are in good agreement and support each other. For instance, it is shown that for fully exchanged H-MOR, the distribution of Brønsted hydroxyls between main channels and side pockets is approximately 2 : 1. On partial ion exchange Na-MOR → HNa-MOR, protons are first introduced into main channel sites, with Na remaining in the side pockets.

INTRODUCTION

The zeolite mordenite forms the basis for commercial catalysts for paraffin and xylene isomerisation. The mordenite is used in the partially dealuminated form in the case of paraffin isomerisation, whereas for xylene isomerisation, samples containing a certain number of sodium ions are particularly successful. Clearly, the nature and the number of active acid sites are important parameters in determining the effectiveness of the catalyst.

FTIR and NMR spectroscopy are usually used to study Brønsted acid sites in various mordenite materials (1, 2). ^{27}Al MAS NMR can provide information on the ratio of the framework/extraframework aluminium atoms (3); combined with chemical analysis and assuming that every framework aluminium generates a Brønsted acid site, their number can be determined. ^{29}Si MAS NMR, according to the literature, does not give a reliable $(Si/Al)_f$ ratio in treated mordenite samples because the peak due to silanol groups overlaps with the Si(1 Al) peak (4). Therefore, it is applied less frequently.

Extensive studies of acidity in mordenites by infrared spectroscopy have been performed using pyridine as a probe molecule. The number of acid sites is estimated on the basis of the intensities of characteristic bands for pyridine interacting with Brønsted sites at around 1545 cm^{-1}, and with Lewis sites at around 1454 cm^{-1} (5–7). However, this method has natural limitations such as: only a certain number of pyridine molecules can be adsorbed; diffusion limitations are possible; sites located in the side pockets might not be accessible.

Another approach that can be employed is analysis of the hydroxyl band. Recently it has been shown that the hydroxyl band of H-mordenite is complex and consists of two overlaid components, a high frequency (HF) peak at around 3612 cm^{-1}, due to the hydroxyls vibrating in the main channels, and a low frequency (LF) peak at around 3585 cm^{-1}, due to the hydroxyls vibrating in the side pockets (8, 9). The bands are not resolved and only the application of special techniques such as second derivative or adsorption–desorption of probe molecules permitted a clear separation of the peaks. By now at least six deconvolutions of the complex hydroxyl band in mordenites have been suggested in the literature (8–14). However, the curvefit used by the authors involves a number of variable parameters, the arbitrary setting of which can give completely different results.

In principle, if the curvefit has been performed reliably and extinction coefficients have been measured, the following information should be obtained:

1. Overall number of Brønsted acid sites in the sample;
2. Their distribution between main channels and side pockets.

Thus, this paper aims to

1. Develop a reliable procedure for deconvolution of the complex hydroxyl band in mordenites;
2. Determine extinction coefficients for the HF and LF components;
3. Perform quantification (number and distribution) on a series of mordenites containing different amounts of extraframework aluminium and sodium;
4. Compare the results obtained with those from ^{27}Al MAS NMR in order to assess the degree of credibility.

[1] Corresponding author. E-mail: MAKAROVA@SIOP.SHELL.NL.

0021-9517/97 $25.00

EXPERIMENTAL

Samples

The starting sodium mordenite (Si/Al = 5.9) was supplied by Zeolyst International. A fully exchanged ammonium mordenite E-1 was prepared by ion exchange with excess ammonium chloride solution (10 g sodium mordenite exchanged twice with 500 ml 2.0 *M* NH_4Cl solution, 1 h, 90°C). A fully exchanged ammonium mordenite E-2 was prepared by a slightly different procedure. It was exchanged three times with 0.2 *M* NH_4NO_3 solution for 1 h at 120°C, followed by two times exchange with 1.0 *M* NH_4NO_3 solution for 1 h at 120°C. Partially exchanged S-1, S-2, S-3 were prepared as follows. 30 g sodium mordenite was slurried in a solution of 30.0 g $NaNO_3$ and 16.4 g NH_4NO_3 in 175.3 g H_2O ($NH_4^+/Na^+ = 0.58$ mol/mol) at 120°C for 2 h, filtered, and washed nitrate free. To change the sodium content the NH_4^+/Na^+ ratio was varied. As a result sodium contents of 1.75, 1.63, 2.02 wt% were obtained for samples S-1, S-2, and S-3, respectively. Sample S-4 was obtained by exchanging sodium mordenite with a limited amount of pure 0.2 *M* NH_4NO_3 solution. It contains 1.75 wt% sodium. Na, Al, Si contents were determined by X-ray fluorescence.

FTIR Measurements

For infrared measurements, a thin self-supporting disc (typically 20 mg, $\rho = 5$–10 mg $\cdot$ cm^{-2}) of a given sample was heated in vacuum to 350–400°C (heating rate 1°/min) and held overnight at the final temperature in an *in situ* FTIR cell, to remove all adsorbed water and ammonia. The sample was subsequently cooled to room temperature or 150°C, and the FTIR spectra were recorded on a Biorad FTS-50 FTIR spectrometer or Cygnus-100 Mattson FTIR spectrometer, between 1300–4000 cm^{-1}, using 100 scans and a resolution of 2 cm^{-1}. To reduce experimental error, measurements were performed up to four times on different disks for each sample, and the averaged spectra, recalculated to the standard thickness of 10 mg $\cdot$ cm^{-2}, were used for subsequent analysis using the GRAMS data analysis package (15).

NMR Measurements

^{27}Al and ^{23}Na solid-state magic-angle-spinning NMR spectra of the hydrated samples were obtained on a Bruker AMX 500 spectrometer (11.7 T), operating at a resonance frequency of 130.3 and 132.3 MHz, respectively. A Bruker 4-mm high-speed MAS probe, free of Al background signal, was used. Samples were spun at a speed of 13.5 kHz, using aluminium-free zirconia rotors. A single pulse sequence was applied. The ^{27}Al and ^{23}Na NMR data were acquired with a small pulse angle ($\pi/12$) to ensure that the data were quantitatively reliable. The acquisition parameters: spectral width (ppm), recycle delay time (s), number of scans and pulse width (μsec) were 4000, 1, 2000, 1.25 for ^{27}Al and 1000, 2, 1600, and 1.5 for ^{23}Na. The ^{27}Al isotropic chemical shifts were referenced to solid aluminium nitride (113.0 ppm), and the ^{23}Na chemical shifts to solid NaCl (7.25 ppm). A line broadening of 25 Hz was applied to all FIDs. In the case of dehydrated materials (for ^{23}Na MAS NMR only), the samples were evacuated at 400°C overnight, the ampules were sealed and spun at 4 kHz; a recycle delay of 10 s was used.

RESULTS AND DISCUSSION

1. FTIR Characterisation of Brønsted Acidity in Mordenites

1.1. Peak fitting of FTIR spectra of Brønsted OH groups. Decomposition of complex bands in infrared spectra is possible using various curve fitting programs that are now generally available (e.g., Ref. (15)). However, as in all fitting programs, care needs to be taken with the analysis because the best fit will obviously depend on the starting values, and in cases where a multitude of solutions are possible, the algorithm tends to converge to the one closest to the starting parameters. Correct choice of starting parameters (and hence, legitimate use of curve fitting) requires:

1. Accurate determination of the number of peaks;
2. Knowledge of the true peak shapes (e.g., Gaussian, Lorentzian, etc.);
3. Approximate estimate of peak parameters (e.g., width, height) and/or their degree of freedom.

Unfortunately for the specific case of hydroxyl groups of zeolites, determining these parameters is not trivial. Firstly, the peak shapes may be not very symmetrical and might not be easily described with a simple immediately available function. Secondly, any single peak might be intrinsically inhomogeneous due, for example, to differences in the Al content of the second coordination sphere, variation in bond angles, presence of extraframework aluminium. Therefore the actual peak position and peak width will depend on the history of the sample.

The difficulties are illustrated in Table 1, where it is seen that at least six attempts have been reported for the deconvolution of the complex hydroxyl band in mordenite (8–14)—with a large variation in the fitting parameters applied. Clearly, for an instructive comparison of a series of mordenites and mordenite-based catalyst materials, a consistent approach to the fitting procedure is required. Thus, one of the aims of the present study is to determine reliable restrictions on the starting parameters for fitting in order to obtain a standard and reproducible decomposition of the hydroxyl region in H-mordenite. This will be further used for determination of the extinction coefficients and, finally, for quantification of the number and distribution

TABLE 1

Parameters for the Deconvolution of the Hydroxyl Region of H-Mordenite; Literature Results

Ref.	Si/Al	T/°C[a]	ν	Deconvolution						I(HF)/I(LF)[b] approx.
				ν(HF)	FWHM	Type	ν(LF)	FWHM	Type	
10, 11	5	−163 to −173	3609	3612	32	G[c]	3585	—	L[c]	2:1
12	10	−173	3610	3612	—	G[c]	3585	40–42	L[c]	1:1
9	10	−163	3614	3616	32	G	3590	44	G	2:1
13	10	−163	3616	3618	—	G	3600	—	L	1:1
8	7.7	25	3607	3612	—	nat.[d]	3585	—	nat.[d]	2:1
14	10	25	3614	3617	30	G	3590	36	G	2:1

Note. G and L are Gaussian and Lorentzian lineshapes.
[a] Temperature of spectrum acquisition.
[b] Approximate ratio of the peak intensities for HF and LF bands.
[c] The line shape is suggested from the published figures.
[d] "Natural" line shape.

of Brønsted acid sites in mordenite and mordenite-based catalyst materials.

1.2. Deconvolution of the spectrum of the standard sample. First a deconvolution procedure has been applied to mordenite containing no extraframework aluminium (see ^{27}Al MAS NMR spectrum in Fig. 4a later) or sodium, E-1, which we take as a standard sample for FTIR measurements. Use of the second derivative allows determination of the approximate peak positions within the complex hydroxyl band. These values are used as initial values for curve fitting. A (65% Lorentzian + 35% Gaussian) peak shape is applied for these two components. The reason for this choice is as follows. It has been reported that a Gaussian peak shape gives the best fit for the high frequency wing of the band, whereas a Lorentzian fit is better for the low frequency part (13). However, we believe that the peak shape for both components should be kept the same—in order to enable the relative areas of the two components to be correctly determined. For this reason a hybrid L/G function for both components is preferred. This choice is further supported by the fact that for zeolite Y, where the HF and LF components are much better separated than in mordenite, the shape of both components was analysed and shown to be close to a 65/35 L/G function (16). Peak widths and peak heights are allowed to vary freely.

Fixed positions for the peaks did not provide a satisfactory fit. Consequently, it was decided to hold the LF peak position fixed and to allow the HF peak position to vary. This decision is based on the empirical observation for mordenites, that when the material is modified in some way, the position of the HF component is significantly affected (8, 17). For instance, it was clearly shown that variation of the total amount of Brønsted sites by ion exchange, caused a change in position of the hydroxyl band in mordenite in the range 3607–3622 cm^{-1} (17). During the curve fitting procedure, the HF band shifts downwards by 2 cm^{-1} and reaches an optimised position. A curve fit obtained under these conditions is shown in Fig. 1.

1.3. Extinction coefficients. The next step is the determination of the distribution of the Brønsted hydroxyls between main channels (HF) and side pockets (LF). It is known that the extinction coefficient increases when the OH band becomes perturbed by hydrogen bonding with various bases or by the electric field of the framework oxygens in the zeolitic rings of small size (18–20). An empirical correlation between the value of the shift due to the perturbation and the increase in absorbance is given elsewhere (21):

$$\varepsilon(\mathrm{LF}) = (1 + 0.018\Delta\nu/\mathrm{cm}^{-1}) \cdot \varepsilon(\mathrm{HF}).$$

For the shift of ~28 cm^{-1} the value of the increase is 1.5. As a consequence, the fraction of HF and LF acid sites may

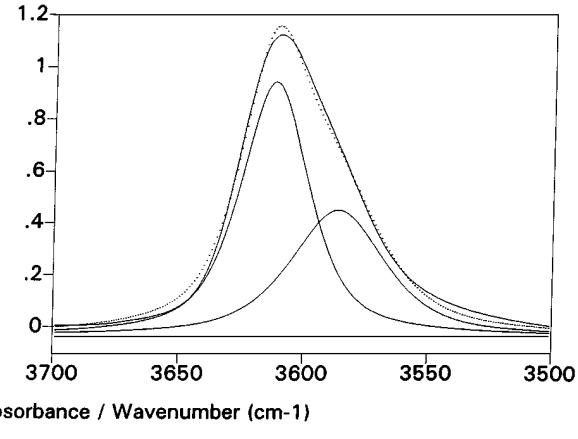

FIG. 1. Deconvolution of the complex hydroxyl region of FTIR spectrum of H-mordenite. Sample E-1. Experimental spectrum and deconvolution: ———; simulated spectrum . . . .

be expressed as

$$\%\text{main channel} = \frac{A(\text{HF})}{A(\text{HF}) + A(\text{LF})/1.5},$$

$$\%\text{side pockets} = \frac{A(\text{LF})/1.5}{A(\text{HF}) + A(\text{LF})/1.5}.$$

The same method was used previously for determination of the distribution of Brønsted hydroxyls between supercages and β-cages in zeolite HY (21). The distribution (%HF : %LF) determined at room temperature is 69% : 31%.

To determine the extinction coefficient, the intensities for the peaks in the deconvoluted spectrum in Fig. 1 have been used. The spectrum represents an average for three different measurements corresponding to $\rho = 10\ \text{mg} \cdot \text{cm}^{-1}$. According to Beer's law,

$$A = \varepsilon \cdot N \cdot \rho$$

where A is absorbance in a.u. cm^{-1}; ε is the extinction coefficient in $\text{cm} \cdot \mu\text{mol}^{-1}$; N is concentration of the active sites in $\text{mmol} \cdot \text{g}^{-1}$; ρ is the thickness of the sample in $\text{mg} \cdot \text{cm}^{-2}$. This sample contains 2.33 $\text{mmol} \cdot \text{g}^{-1}$ Brønsted sites (based on chemical analysis for Na, Al, and the absence of extraframework Al as determined by NMR). This then corresponds to 1.61 $\text{mmol} \cdot \text{g}^{-1}$ in the main channels and 0.72 $\text{mmol} \cdot \text{g}^{-1}$—in the side pockets. Thus,

$$\varepsilon(\text{HF}) = 2.5\ \mu\text{mol} \cdot \text{g}^{-1},$$

$$\varepsilon(\text{LF}) = 3.8\ \mu\text{mol} \cdot \text{g}^{-1} \quad \text{(at room temperature)}.$$

1.4. Standardised deconvolution procedure. Although the approach described above provides a reasonable fit for a standard sample, it cannot be automatically extended to other samples. The reason is that both HF and LF peaks are intrinsically inhomogeneous and can change their positions, symmetry, and peak width, depending on the pretreatment conditions. Therefore, we have chosen to fit each of the peaks (HF and LF) with a set of three primary components: one at the peak position determined for the standard sample, and the other two shifted by $\pm 5\ \text{cm}^{-1}$. The peak shape is 65%L + 35%G; FWHM is 33 cm^{-1} for primary components of the HF peak and 45 cm^{-1} for primary components of the LF peak. The degree of flexibility in the primary components' positions and their FWHM are justified by the previous experiments on ammonia thermodesorption and sodium ion exchange (8, 17).

From a mathematical point of view this procedure is similar to expressing each peak as a series (only three members in our case) and does not have a physical meaning. After deconvolution, the first three fitted primary components are summed to obtain a HF peak and the second three are summed to obtain a LF peak. This approach has two major advantages:

- It provides the necessary flexibility in peak position, width, and symmetry within the limits of the standard deconvolution program and prevents the user from a biased choice of the fitting parameters.
- It provides a stable final deconvolution, independent on the input intensities of the primary components, since any possible redistribution of intensities within each set of three primary components, depending on the closest minimum, does not affect each sum of three.

Based on the above, we can now define the required input parameters to provide a general deconvolution method for the hydroxyl region of H-mordenite (even in the presence of extraframework aluminium) using a curve fitting program.

1. Choice of baseline and spectral region. This should be wide enough (at least 5 FWHM) and kept constant for all the spectra undergoing curve fitting. We propose using the 3500–3700 cm^{-1} region and a linear 2-point baseline, so that absorbance intensities corresponding to these and point equal zero.

2. Number of peaks to include in the fit. This is limited to three primary components to express the HF peak, three primary components to express the LF peak, plus an additional peak at ~3660 cm^{-1} for extraframework $\text{Al}_x(\text{OH})_y$ species, if present. Therefore, seven peaks in total.

3. Peak shape. This is fixed to 65% Lorentzian + 35% Gaussian, for all the peaks, as justified above.

4. Peak positions, peak width (FWHM), at room temperature. Primary components to express the HF peak: 3617, 3612, 3607 cm^{-1}, FWHM = 33 cm^{-1} (fixed); primary components to express the LF peak: 3591, 3586, 3581 cm^{-1}, FWHM = 45 cm^{-1} (fixed); the peak at 3660 cm^{-1} with FWHM of 20 cm^{-1} for $\text{Al}_x(\text{OH})_y$ species, where present (varied).

5. Peak heights. These are not fixed, although the initial values are set 2 : 1 for the primary components of the HF peak to those for the LF peak. An illustration of the input file is given in Fig. 2. The overall intensity of the input components should be close to that of the spectrum to be fitted.

1.5. Application to the series of mordenite samples. The procedure described above has been applied in a consistent manner to other mordenite samples. Deconvoluted spectra are given in Fig. 3. The distribution of the hydroxyls between the main channels and side pockets, and the overall amount of acid sites are presented in Table 2. Note that the deconvolution for the standard sample, done on the basis of 1-peak fitting for both HF and LF peaks (Parts 1.2 and 1.3) and by 3-component fittings for each, as described in 1.4 give almost the same distribution of Brønsted hydroxyls between main channels and side pockets.

In the fully ion-exchanged mordenites, the distribution of Brønsted hydroxyls between main channels and side pockets is close to 2 : 1. Furthermore, sodium, if present,

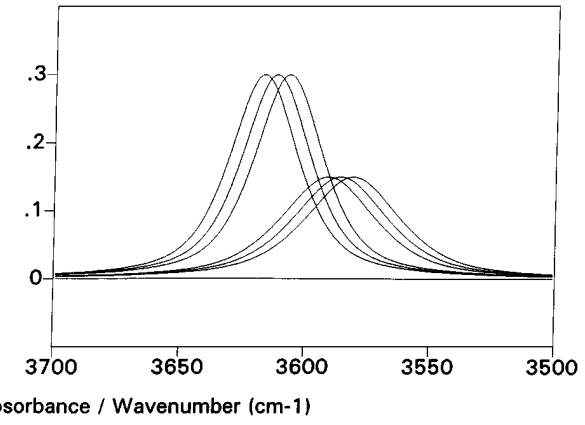

FIG. 2. An input file for standardised deconvolution of the complex hydroxyl region in FTIR spectra of mordenites (see text for explanations).

substitutes protons mainly in the side pockets. Therefore, it has been directly demonstrated that partially exchanged samples have a different distribution of acid sites between main channels and side pockets, as compared to fully ion-exchanged mordenites. This approach also enables the decrease in the overall acidity resulting from partial framework dealumination during ion exchange to be monitored. It will be shown further that these results correlate with NMR data.

2. NMR characterisation of mordenites. ^{27}Al MAS NMR is usually used for the determination of extraframework aluminium. A spectrum in the general case consists of three peaks: one peak at 55 ppm which is assigned to structural tetrahedral aluminium; a peak at ~30 ppm which is often assigned to pentacoordinated, nonframework aluminium oxide; and a peak at 0 ppm which is due to nonframework, octahedral aluminium (4). A complication for the quantitative measurements is that the line shape can be complicated by quadrupolar broadening; therefore a mathematical deconvolution of the spectrum requires rigorous knowledge of the quadrupolar coupling constant and the asymmetry parameter, when quadrupolar broadening is present.

To quantify the spectra we used a different approach to that reported in the literature. The sample S-1 which contains tetrahedral aluminium only (see Fig. 4c for ^{27}Al MAS NMR spectrum), was used as a standard sample for NMR measurements; this provides the line shape for the component at 55 ppm. The percentage of this component in the overall complex spectra of the other samples was considered to be the percentage of framework aluminium amongst all the aluminium atoms present in the material. Experimental ^{27}Al MAS NMR spectra, together with the fitted component at 55 ppm are shown in Fig. 4. Assuming that all the sodium atoms in the sample compensate framework aluminium and there is no cationic aluminium in the sample, the amount of Brønsted sites can be calculated as follows:

$$2.33 \times [\%I(\text{Al, 55 ppm})/100 - \text{Na/Al(mol. ratio, chem. anal.)}] \text{ mmol/g.}$$

The results obtained in this manner are given in Table 3. The NMR results obtained are in accord with the results obtained by FTIR. Samples which possess extraframework aluminium according to NMR, also demonstrate the band at ~3660 cm^{-1} in the FTIR spectra due to $Al_x(OH)_y$ extraframework species. The values for the overall Brønsted acidity, determined by both methods are in a good agreement (Tables 2 and 3).

An attempt was made to employ ^{23}Na MAS NMR to examine the distribution of sodium cations, where present, between main channels and side pockets. Hydrated samples demonstrate a sharp peak at −10 ppm which after a prolonged calcination under vacuum is transformed into a much broader peak at −20 ppm, in accordance with literature results on Na-ZSM-5 (22). However, no significant differences were observed between the samples containing sodium in the side pockets only, on one hand, and the samples with sodium in both main channels and side pockets, on the other hand. This shows that ^{23}Na MAS NMR is not

TABLE 2

FTIR Characterisation of the Brønsted Acidity in Mordenite Samples

No.	Sample	Na[a] wt%	Extra framework Al	Proton distribution (norm.) Main (%)	Side p. (%)	Acidity[b] mmol/g
1	E-1	0	−	68	32	2.36
2	E-2	0	+	68	32	0.97
3	S-1	1.75	−	93	7	1.63
4	S-2	1.63	+	91	9	1.16
5	S-3	2.02	+	89	11	0.61
6	S-4	1.75	+	90	10	0.49

Note. +, present; −, absent.
[a] From chemical analysis.
[b] Experimental error ±9%.

TABLE 3

Brønsted Acidity in Mordenite Samples According to ^{27}Al MAS NMR Results

No.	Sample	Na/Al	%Al (tetra)[a]	mmol/g
1	E-1	0	100	2.33
2	E-2	0	39	0.91
3	S-1	0.33	100 (standard)	1.56
4	S-2	0.31	84	1.23
5	S-3	0.38	63	0.58
6	S-4	0.33	61	0.65

[a] Experimental error ±7%.

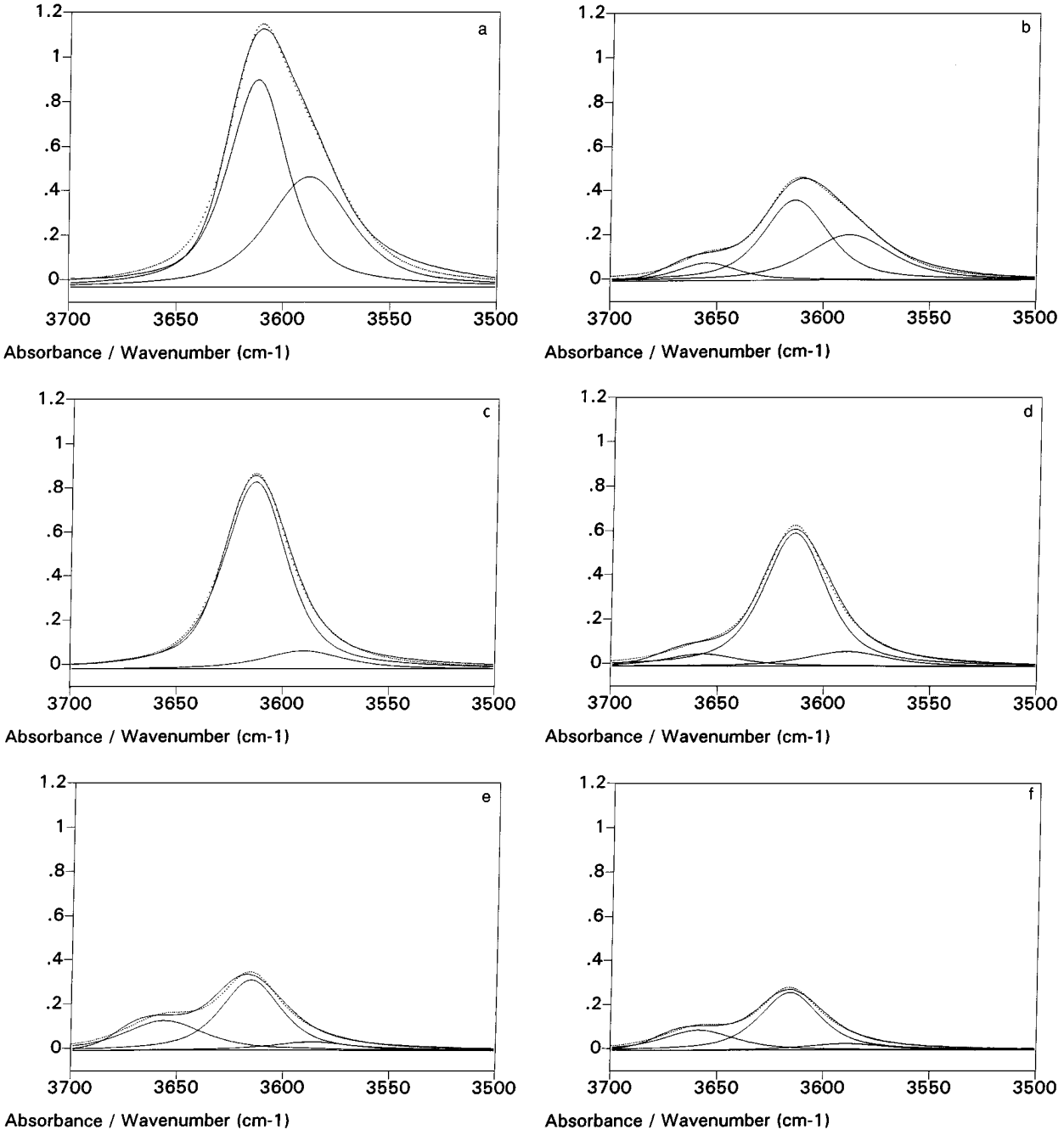

FIG. 3. Deconvolution of the hydroxyl region of FTIR spectra of various mordenite samples, based on the standardised procedure: (a) E-1; (b) E-2; (c) S-1; (d) S-2; (e) S-3; (f) S-4. Experimental spectra and deconvolution: ———; simulated spectra . . . .

a suitable tool for determining the distribution of Na ions between the various sites.

CONCLUSIONS

A comprehensive study to quantify Brønsted acid sites in mordenite samples containing sodium and extraframework aluminium has been performed using Fourier transform infrared and solid-state NMR. A standardised deconvolution procedure of the complex hydroxyl region of mordenites has been developed and extinction coefficients for the HF and LF peaks determined. The results obtained by NMR and FTIR are in good agreement and strongly support each other. This enhances the credibility of the quantification performed by using each of the methods.

The new deconvolution procedure allows reliable determination of the distribution of the Brønsted hydroxyls between main channels and side pockets, even in the presence

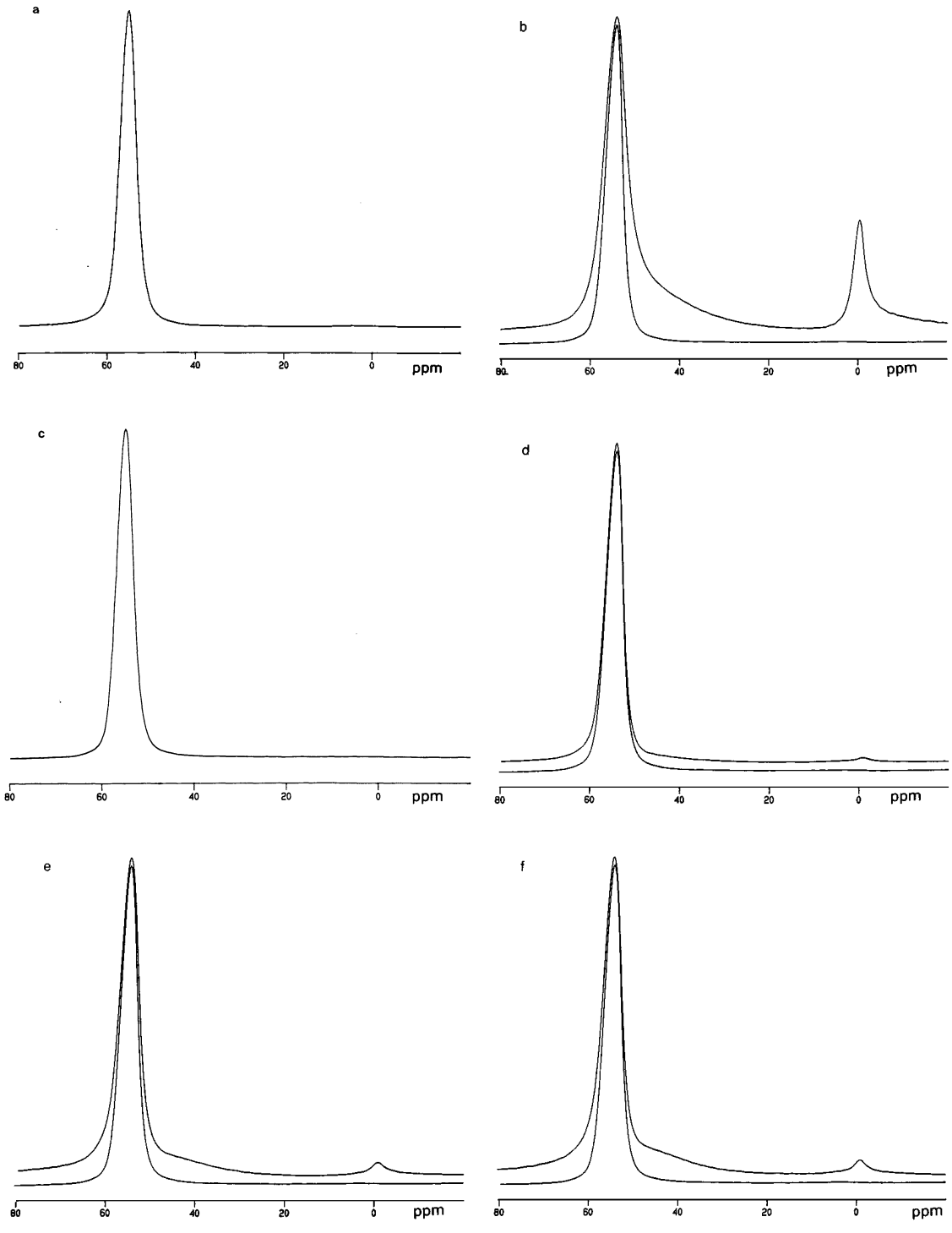

FIG. 4. Experimental ^{27}Al MAS NMR spectra of various mordenite samples, together with the fitted component at 55 ppm (where appropriate): (a) E-1; (b) E-2; (c) S-1; (d) S-2; (e) S-3; (f) S-4.

of extraframework aluminium and/or residual sodium. For instance, for a fully ion-exchanged mordenite the distribution of the hydroxyls is close to 2 : 1. Furthermore, it is shown that during ion exchange Na-MOR → HNa-MOR, Na cations in the main channels are exchanged in the first instance.

Combining catalytic results with FTIR monitoring of acid sites distribution and NMR/FTIR monitoring of the overall

Brønsted acidity, as described here, may provide a simple, effective tool to understand and control catalyst quality and reproducibility of catalyst manufacture in as-synthesised and dealuminated samples. Furthermore, it can be applied more generally for fine-tuning of the number and distribution of acid sites in other multichannel systems.

ACKNOWLEDGMENT

The authors thank Shell International Chemicals for permission to publish this paper.

REFERENCES

1. Van Niekerk, M. J., Fletcher, J. C. Q., and O'Connor, C. T., *J. Catal.* **138**, 150 (1992).
2. Wu, P., Komatsu, T., and Yashima, T., *J. Phys. Chem*. **99**, 10923 (1995).
3. Engelhardt, G., and Michel, D., "High Resolution Solid-State NMR of Silicates and Zeolites." Wiley, New York, 1987.
4. Miller, J. T., Hopkins, P. D., Meyers, B. L., Ray, G. J., Roginski, R. T., Zajac, G. W., and Rosenbaum, N. H., *J. Catal*. **138**, 115 (1992).
5. Karge, H. G., *Z. Phys. Chem. Neue Folge* **76**, 133 (1971).
6. Karge, H. G., *Z. Phys. Chem. Neue Folge* **122**, 103 (1980).
7. Kojima, M., Rautenbach, M. W., and O'Connor, C. T., *J. Catal.* **112**, 505 (1988).
8. Zholobenko, V. L., Makarova, M. A., and Dwyer, J., *J. Phys. Chem*. **97**, 5962 (1993).
9. Wakabayashi, F., Kondo, J., Wada, A., Domen, K., and Hirose, C., *J. Phys. Chem*. **97**, 10761 (1993).
10. Borida, S., Lamberti, C., Geobaldo, F., Zecchina, A., Turnes Palomino, G., and Otero Areán, C., *Langmuir* **11**, 527 (1995).
11. Geobaldo, F., Lamberti, C., Ricchierdi, G., Bordiga, S., Zecchina, A., Turnes Palomino, G., and Otero Areán, C., *J. Phys. Chem*. **99**, 11167 (1995).
12. Maache, M., Janin, A., Lavalley, J. C., and Benazzi, E., *Zeolites* **15**, 507 (1995).
13. Wakabayashi, F., Kondo, J., Domen, K., and Hirose, C., *Bull. Natn. Sci. Mus. Tokyo Ser. E* **17**, 19 (1994).
14. Wakabayashi, F., Fujuno, T., Kondo, J. N., Domen, K., and Hirose, C., *J. Phys. Chem*. **99**, 14805 (1995).
15. "Grams/386." Microsoft Corporation, 1985–1991.
16. Jacobs, P. A., and Uytterhoeven, J. B., *J. Chem. Soc. Faraday Trans. I* **69**, 359 (1973).
17. Datka, J., Gil, B., and Kubacka, A., *Zeolites* **15**, 501 (1995).
18. Pimentel, G. C., and McMellan, A. L., "The Hydrogen Bond." Freeman, San Francisco, 1960.
19. Joesten, M. D., and Schaas, L. J., "Hydrogen Bonding." Dekker, New York, 1974.
20. Jacobs, P. A., and Mortier, W. J., *Zeolites* **2**, 226 (1982).
21. Makarova, M. A., Ojo, A. F., Karim, K., Hunger, M., and Dwyer, J., *J. Phys. Chem*. **98**, 3619 (1994).
22. Scholle, K. F. M. G. J., Ph.D. thesis, 1985, p. 95.